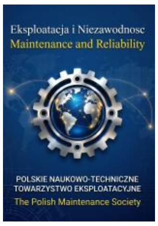


**Eksploatacja i Niezawodnosc - Maintenance and Reliability**

Volume 29 (2027), Issue 2

https://ein.org.pl

The Polish Maintenance Society

# Influence of rotor blade rotational speed on the spectrum and emission level of noise in the rotating system of the dual-use small Wabik helicopter

Piotr Wróblewski[1,2*], Stanisław Kachel[1], Łukasz Kiszkowiak[1]

[1] Faculty of Mechatronics, Armament and Aerospace, Military University of Technology, Warsaw, Poland
[2] Faculty of Engineering, University of Technology and Economics H. Chodkowska in Warsaw, Poland
* Corresponding Author: piotr.wroblewski@wat.edu.pl

*Received: 31 May 2026*
*Revised: 13 June 2026*
*Accepted: 11 July 2026*
*Online: 17 August 2026*



**Abstract**

This article investigates the influence of rotor-head rotational speed on the overall A-weighted noise level and the 1/3-octave spectral structure of the prototype dual-use Wabik helicopter. The novelty of the work is the separation of mechanical hub/drive noise from blade-generated aerodynamic noise for a custom three-bladed rotor system tested at 1000, 1250, and 1500 RPM under identical outdoor conditions. For the configuration without blades, the energetic mean LAeq increased from 81.76 dB to 85.56 dB and 88.28 dB, respectively. After installing the rotor blades, LAeq rose from 86.50 dB at 1000 RPM to 92.53 dB at 1250 RPM and 98.45 dB at 1500 RPM, corresponding to an increase of about 12 dB and an almost sixteenfold rise in acoustic energy. The dominant spectral bands shifted from 2.5 kHz through 1 kHz to 800 Hz, while the 0.8–3 kHz range became critical for detectability and operator safety. These results provide quantitative guidance for selecting rotor operating ranges, improving blade geometry, and reducing the acoustic signature of small rotorcraft.

**Keywords:** *aerodynamic noise, rotor blade rotational speed, helicopter, 1/3-octave spectrum, unmanned aerial vehicles.*

*Article citation:*
Wróblewski P, Kachel S, Kiszkowiak Ł, Influence of rotor blade rotational speed on the spectrum and emission level of noise in the rotating system of the dual-use small Wabik helicopter, Eksploatacja i Niezawodnosc – Maintenance and Reliability 2027: 29(2) http://doi.org/10.17531/ein/225750

## Highlights

- The 0.8–3 kHz range became critical for detectability and operator safety.
- Rotor blades are the main source of aerodynamic noise.
- Rotor operating conditions strongly influence the acoustic signature of the helicopter.

## 1. Introduction

In recent years, a very rapid development of dual-use unmanned aerial vehicles and light rotorcraft structures has been recorded. This is of particular importance in both the civil and military areas. This became especially significant at the moment of the outbreak and during the armed conflict in Ukraine, where reconnaissance and strike unmanned aerial vehicles constitute one of the main elements of the modern battlefield [1,2]. The very wide application of unmanned aerial vehicles led to the parallel development and investigations of counter-drone systems and passive detection methods. In particular, the area of acoustic detection is also developing, which does not require emission of its own signal and is more difficult to jam [3,4]. In work [5] it was presented that the war in Ukraine led to significant changes in the manner of conducting armed operations through the mass use of unmanned aerial vehicles. Contemporary small aircraft perform reconnaissance, combat, and logistic functions, and particularly important significance is held by low-cost FPV designs, which make it possible to neutralize costly military equipment of the opponent. The authors indicate that the increased number of unmanned aerial vehicles on the battlefield significantly reduced the possibilities of concealing soldiers and strategic objects and increased the effectiveness of precise combat strikes both on the front line and at large distances deep in the opponent's operational rear [5]. At the same time, counter-drone systems are developing dynamically, including kinetic means and electronic warfare. An important problem in this case remains the cost disproportion between the relatively inexpensive production of small aircraft and the costly systems for their neutralization [5].

At present, the use of small short-range and long-range aircraft has become the most important element of the modern battlefield. Therefore, the development of such designs and the improvement of their operational parameters become essential for many NATO member states.

Contemporary military operations require design solutions for small aircraft with a reduced detectability signature. Although basic radar and radio systems may be susceptible to jamming, the acoustic signature of small rotorcraft remains an important parameter from the point of view of enemy detection [4,6]. It is emphasized in the literature that the acoustic characteristics of small aircraft depend strongly on rotor rotational speed, blade geometry, and environmental conditions [3,6]. Investigations on the acoustic characteristics of a propeller in a small aircraft as a function of propeller blade geometry were carried out in work [7]. The investigation showed that propeller diameter has a greater influence on the generated thrust force than its pitch. Moreover, an increase in blade pitch makes it possible to obtain greater thrust force at high engine rotational speeds at the expense of greater thermal loading of the engine [7]. The selection of the propulsion propeller should always be individually matched to the power and torque characteristics of the reciprocating internal combustion engine and to the intended use of the aircraft. In this case, such selection should take into account not only the maximum thrust force, but also the torque parameters. The work also presents the construction of a modern test stand enabling a detailed assessment of the influence of propeller geometry on the operational parameters of the propulsion system of unmanned aerial vehicles [7]. In work [8] it was demonstrated that the main source of noise in ultralight aircraft with two-stroke engines is the propeller directly coupled to the crankshaft, and the sound intensity level increases with increasing engine rotational speed. The investigations confirmed that an appropriate selection of propeller geometry makes it possible to obtain a more favorable compromise between generated thrust force and noise emission. The work emphasizes the importance of proper selection of propulsion system operating parameters in order to reduce acoustic impact, particularly in flights carried out near inhabited areas [8]. Such parameters are particularly important in military operations in order to limit the emission of generated noise.

Noise generated by rotor systems has a complex character and includes aerodynamic, mechanical, and blade–vortex interaction (BVI) components [9,10]. These phenomena lead to the occurrence of characteristic maxima in the frequency spectrum, particularly in the medium-frequency range. Investigations on helicopter rotor noise showed that an increase in rotational speed causes a nonlinear increase in acoustic emission, particularly in bands corresponding to the fundamental blade-passage frequencies [9]. In work [11], a detailed acoustic analysis of unmanned aerial vehicles under environmental conditions was carried out, indicating that multirotor designs differ significantly in terms of noise emission depending on the number of propellers. It was shown that small aircraft of X6 configuration generate higher A-weighted sound levels and higher acoustic background levels than X4 designs. This is directly related to the number of operating rotors [11]. It is important that the spectral analysis revealed characteristic frequency maxima, most often occurring in the 50 Hz, 200 Hz, and 315 Hz bands, which may be regarded as typical for the operation of propellers of small UAVs [11]. Moreover, it was established that aircraft of the same type are characterized by a similar acoustic signature. These results confirm that the spectral analysis of propeller noise constitutes an important tool both for the detection and identification of unmanned aerial vehicles [11].

It should be remembered that each aircraft and its propulsion system, including the power and torque characteristics of the internal combustion or electric engine, as well as the geometry and number of propulsion propellers, generate an individual acoustic spectrum characteristic. Therefore, for prototype designs, test-stand investigations must always be carried out in order to improve the operational parameters of the small aircraft design.

Investigations of noise levels require the adoption and application of appropriate measurement procedures. In experimental investigations, the parameter, i.e., the equivalent level $L_{\mathrm{Aeq}}$, and the parameter with time weighting (e.g., $L_{\mathrm{AS}}$), are used in accordance with ISO 1996-1 [12] and the requirements concerning measuring devices specified in IEC 61672-1 [13]. In investigations concerning noise levels for civil aviation, the legal standard is the ICAO documents, including

Annex 16 and the Environmental Technical Manual [14,15]. It specifies in great detail the principles of measurement and assessment of aircraft noise emission levels. The strategy and specific guidelines concerning noise reduction were included in the ICAO study concerning the strategy for limiting acoustic impact [16].

In times of the active armed conflict in Ukraine, the issue of noise emission for small aircraft is becoming a very important issue, in particular in the scope of practical guidelines for the design and construction of aircraft in a combat role. Small aircraft are commonly used as reconnaissance and combat means [1,2]. Despite this, systems for their detection and neutralization are also being developed, including solutions based on the analysis of acoustic signals [3,4]. This is particularly being developed in aircraft detection and neutralization systems within counter-drone systems. In such realities, the limitation of noise emission in specific bands may affect the reduction of aircraft detectability, whereas the spectrum analysis may serve for the identification of the rotor type and operating parameters [6].

In work [17], it was presented that small unmanned aerial vehicles play a significant role in contemporary warfare. The use of these systems makes it possible to conduct reconnaissance effectively and to carry out precise strike operations with explosive payloads. The development of unmanned aerial vehicle systems leads to greater autonomy in armed operations. The work also drew attention to the particular needs in the scope of increasing the production capacities of unmanned aerial vehicles and creating new solutions for military purposes.

Drone control systems, including those of small dual-use helicopters, are technically very complex and must be developed in the scope of precise control and possible cyberattacks. It is also worth mentioning that at present an increasing number of studies and defense enterprises are working on drone systems supported by artificial intelligence. This is especially important in the case of the autonomous flight of a dozen or so aircraft simultaneously to their target.

In the context of the rapid development of prototype designs, often created within a short design cycle, it becomes particularly important to carry out comparative investigations enabling precise determination of the influence of selected design and operational parameters on noise emission. This applies in particular to rotor rotational speed, which directly determines the acoustic energy generated by the aerodynamic system.

In work [18], hybrid propulsion systems for unmanned aerial vehicles were described, combining an internal combustion engine with an electric motor, which makes it possible to increase flight endurance, range, and energy utilization efficiency in comparison with exclusively electric or internal combustion propulsion. Such solutions are particularly useful in specialist and dual-use drones. It is also worth building and creating new test stands for rapid testing of prototype engines intended for drone propulsion in various configurations [19]. In work [20], issues of aerodynamic design and optimization of propellers for multirotor configurations were described, demonstrating the significant influence of blade geometry on aerodynamic efficiency and the flight performance parameters of unmanned aerial vehicles. This is of particular importance for noise emission. In work [21], the development of composite technologies based on experience gained from helicopter rotor blade structures was described, indicating that both aerodynamic optimization and the selection of modern composite materials are of key importance in the design of propellers and rotors used in unmanned aerial vehicles. These are important aspects concerning propeller selection for different aircraft.

Newer investigations confirm that rotor and propeller noise in UAV systems is governed by both tonal components related to the blade-passing frequency and broadband aerodynamic components, while rotational-speed fluctuations may additionally generate middle-frequency tonal noise [22,23]. Recent outdoor measurements also show that the spectral structure of UAV acoustic signatures is important for detection range and signal-to-noise ratio under field conditions [24]. Moreover, current diagnostic research demonstrates that acoustic signatures of UAV propeller blades can be used to identify operating state and blade condition, which supports the practical value of detailed spectral analysis in the present work [25].

The main goal of this study is to quantify how rotor-head rotational speed changes the overall A-weighted noise level and the 1/3-octave spectral distribution of the Wabik rotor system under repeatable test-stand conditions. The scientific novelty lies in the direct comparison of the same prototype drive in two configurations, with and without rotor blades, which enables the mechanical contribution of the hub/drive system to be separated from the blade-generated aerodynamic component.

The objective of the present work is the analysis of the 1/3-octave spectrum and the equivalent noise level for the prototype Wabik rotor system in the configuration with the rotor and without the rotor, as well as the determination of the influence of rotational speed (1000, 1250, and 1500 RPM) on the spectral structure and the total emission level. The obtained results constitute a basis for further improvement of the design in terms of noise emission reduction and assessment of its potential acoustic detectability under operational conditions.

The novelty of this work is the detailed 1/3-octave spectral analysis of the conceptual Wabik helicopter in the configuration with the rotor and without the rotor at three defined rotational speeds. This makes it possible to determine the influence of the rotor system itself on the structure and level of acoustic emission. In contrast to previous investigations focusing primarily on the analysis of the total noise level, the work carried out a detailed assessment of the distribution of acoustic energy in frequency bands significant from the point of view of passive detection. The investigation results make it possible not only to analyze the operational parameters of the Wabik helicopter design, but also its potential acoustic detectability under operational conditions. This is of particularly significant importance in military applications. Moreover, the adopted research methodology may constitute a basis for further investigations of prototype propulsion systems intended for dual-use unmanned aerial vehicles.

## 2. Research object – the structure of the small aircraft of the Wabik type

The research object is the unmanned helicopter Wabik. It is a rotorcraft platform of low empty mass intended for military and civil applications. The total mass of the structure is approximately 20 kg, with the capability of carrying a payload of approximately 14 kg. The Wabik helicopter enables the integration of optoelectronic heads, observation systems, and specialist sensors, e.g. for the detection of environmental contamination. The maximum flight speed is approximately 120 km/h (depending on the geometry of the rotor blades and the applied propulsion engine), the operational ceiling is 3000 m, with the possibility of increasing it to 4500 m. The theoretical flight endurance of the Wabik helicopter, depending on the amount of fuel and the design of the tanks, is up to 2 hours, which enables covering a distance of more than 200 km without landing. The structure of the aircraft allows autonomous flight, including patrolling designated areas without direct operator interference. This allows increasing its usefulness in reconnaissance tasks, critical infrastructure monitoring, and operations of a dual-use character.

## 3. Methodology of experimental research

### 3.1. Bench tests with the use of the Wabik aircraft

The research was conducted in controlled outdoor conditions, with consideration given to minimizing the influence of environmental disturbances, including background noise and vibrations transmitted through the ground. The measurements were performed in two research configurations: with the rotor installed and without the rotor, which made it possible to determine the direct influence of the blade system on the level and spectral structure of acoustic emission. The measurements were performed for three fixed rotational speeds: 1000, 1250, and 1500 RPM, ensuring stabilization of the operating parameters before the beginning of signal recording. Each measurement was performed under constant geometric and environmental conditions, while maintaining a constant distance of the measuring microphone from the investigated object and a repeatable recording time (Fig. 1).

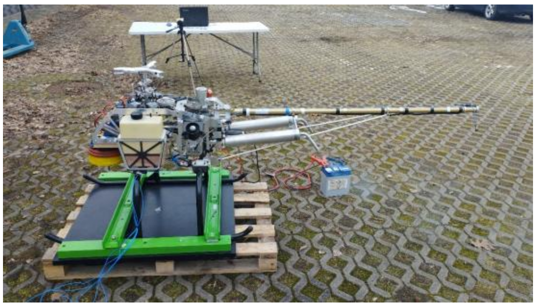

Figure 1. View of the Wabik aircraft with the deployed noise-level measuring apparatus (without rotor).

The height of the Wabik helicopter with the mounting stand is 100 cm up to the central point of the rotor head. The height of the aircraft from the landing skid to the rotor head is 85 cm (Fig. 2). The distance of the digital sound analyzer from the central point of the head was 300 cm. The measuring device was positioned perpendicular to the aircraft on the rotor-head axis.

Figure 2. View of the rotor head of the Wabik aircraft with the belt transmission system and the control system.

The applied measuring apparatus was calibrated in accordance with the applicable metrological standards. The research stand prepared in this way made it possible to conduct measurements in a wide frequency band and to perform spectral analysis in a 1/3-octave division. Such an approach allows identification of the characteristic noise components generated by the rotor system and assessment of the effect of the change in rotational speed and the presence of blades on the energy structure of the acoustic signal. This system also allows assessment of the noise generated by the propulsion system in two configurations, without blades and with blades, with the engine running for 3 rotational speeds of the rotor head. A view of the transmission assembly, which generates an additional source of noise, is presented in Figure 3. The measurement time for each test was 60 seconds. For each of the configurations and rotor-head rotational speeds, 3 measurements of 60 seconds each were performed.

Figure 3. Transmission system of the rotor-head drive of the Wabik aircraft and the load-bearing frame with the fuel tank.

For the readout of the parameters of the Wabik aircraft and for control, the FrSky TANDEM X18SE radio controller was adopted in the test stand (Fig. 4). It is intended for controlling executive processes of unmanned aircraft [26]. The controller operates on ETHOS software. The device is equipped with a built-in internal module with RF parameters TD-ISRM Dual-Band 900 MHz/2.4 GHz. Such a configuration allows simultaneous operation of the control system in two frequency bands [26]. The control set allows obtaining an extremely low system response delay time to the commanded value, on the order of 4 ms, and an effective range of up to 100 km [26]. The adoption of such a control system in this unmanned aircraft allows test operations to be conducted over very long distances for a long time. The controller allows operation of the ACCESS, ACCST D16, and TD protocols [26].

Figure 4. FrSky TANDEM X18SE remote-control system installed in the Wabik aircraft with the possibility of reading head temperatures, supply voltage, and rotor-head rotational speed.

The ETHOS system allows the control process to be conducted in analog and touch mode, as well as the launching of LUA scripts. This makes it possible to introduce advanced control algorithms and telemetry functions. The controller also has a built-in 6-axis gyroscopic sensor, a system of haptic vibration alerts, and the PARA wireless training system [26].

In the research and construction of the Wabik aircraft, the FrSky Hall RPM Sensor ADV rotational-speed sensor [27] was used. The sensor allows non-contact measurement of the rotational speed of rotating elements through detection of the magnetic field generated by a magnet mounted on the rotating element (Fig. 5). In the research, it is used for measurement of the rotational speed of the rotor head and thus the speed of the rotor blades, where the measurement result is read directly from the FrSky TANDEM X18SE set (Fig. 6). The device cooperates with telemetry systems used in RC model aviation and can transmit measurement data to the receiver by means of the FBUS or Smart Port (S.Port) interface [27] (Fig. 6). This sensor may also operate in PWM output mode. The sensor enables measurement of rotational speed in the range from approximately 400 to 60,000 rpm [27]. The dimensions of the sensor module are approximately 18 × 10 mm, whereas the dimensions of the magnet used for rotation detection are 6 × 3 mm [27]. The mass of the sensor is approximately 2.5 g, and the mass of the magnet approximately 0.64 g, owing to which the device may be used in lightweight structures, such as unmanned aerial vehicles or test stands for measurement of rotor operating parameters [27].

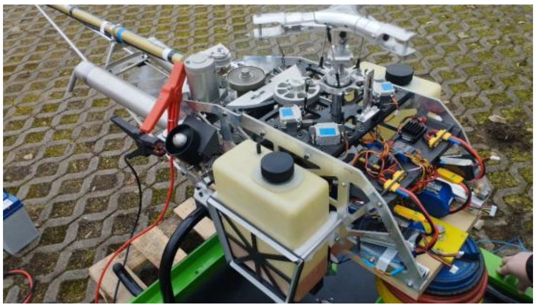

Figure 5. View of the rotor head assembly, the control assembly of the Wabik aircraft with the FrSky Hall RPM Sensor ADV sensor assembly – tests without installed blades.

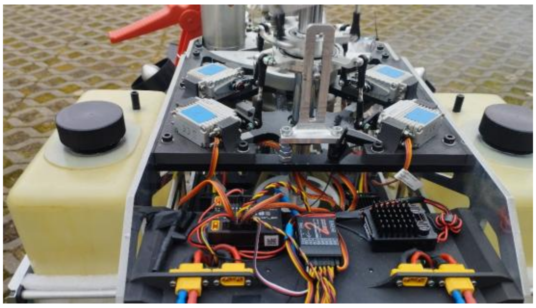

Figure 6. Control assembly of the Wabik aircraft together with the radio information processing system and the power supply system.

In the Wabik helicopter, for tests, a two-cylinder piston internal combustion engine DLE-170 with spark ignition was installed (Table 1). The two-stroke engine system ensures high power density at a low mass of the propulsion unit [28]. The ignition system ensures high operating stability even at high rotational speeds of the engine crankshaft. The carburetor fuel supply system allows, after making minor corrections, stable operation in various load modes with the use of different rotor blades. Owing to the good mass-to-power ratio, the internal combustion engine allows obtaining a very good torque distribution, ensuring stable operation under variable load [28]. After applying appropriate modifications, additional measuring elements may be introduced into the propulsion system, including the engine, such as temperature sensors, shaft speed and position sensors, and many others necessary for conducting experimental research. The engine was additionally equipped with an independent fan cooling system (Fig. 7).

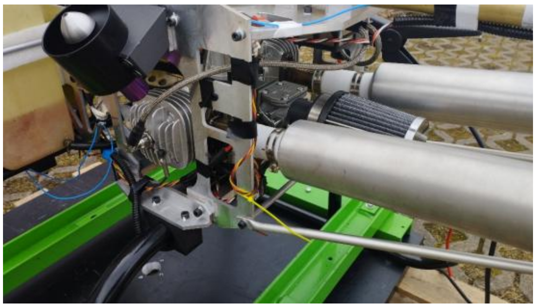

Figure 7. Cooling assembly of the piston internal combustion engine constituting part of the propulsion assembly of the Wabik aircraft.

Table 1. Technical data of the DLE-170 engine [28].

| Model | DLE-170 |
|---|---|
| Type | Two-cylinder, spark ignition |
| Displacement | 170 cm³ |
| Cylinder bore | 52 mm |
| Piston stroke | 40 mm |
| Compression ratio | 9.5:1 |
| Maximum power | 17.5 hp at 9000 rpm |
| Speed range | 1100-9000 rpm |
| Recommended fuel mixture | 30:1 (gasoline:oil) |
| Engine mass | 3550 g |
| Total mass | approx. 4110 g |
| Spark plug | CM6 |
| Recommended ignition voltage | max. 7.4 V |

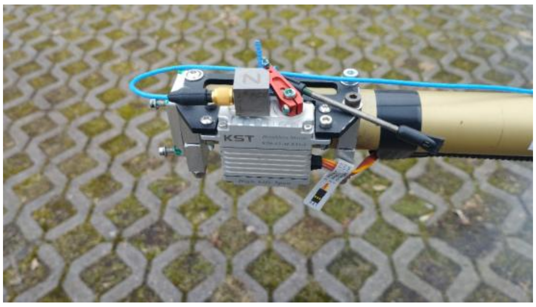


Figure 8. View of the KST X20-12-M-835-HV Brushless digital brushless servomechanism mounted on the rear axis for control of the tail rotor of the Wabik aircraft.

In the structure of the Wabik unmanned helicopter, the KST X20-12-M-835-HV brushless digital servomechanism, intended for operation in systems with high dynamic loads [29], was used (Fig. 8). This servo generates a maximum torque of up to 48 kg·cm (approximately 4.7 N·m) and is characterized by a response time of 0.14 s per 60°, which enables fast and precise control of the angle of attack of the main rotor blades and the elements of the tail system [29] (Fig. 8). This device operates using high-voltage batteries, which allows obtaining a rapid response to the settings commanded by the operator.

During the tests of noise generated by the Wabik helicopter, a three-bladed VARIO rotor blade set was mounted on the VARIO Helicopter rotor head. Its characteristics are presented in Table 2. The rotor-blade dimensions and material data were adopted from the manufacturer's product specification [30].

Table 2. Specification of the VARIO Helicopter rotor blade [30].

| Parameter | Value |
|---|---|
| Blade length | 1090 mm |
| Rotor disk diameter | 2500 mm |
| Root attachment | 22 mm, one mounting hole |
| Blade chord | 75.00 mm |
| Airfoil thickness | 1 mm |
| Mass | approx. 500 g |
| Material | CFRP (carbon fiber reinforced composite) |
| Surface finish | Shark Skin, matte anthracite |
| Symmetry | reflex airfoil, left- and right-hand version (LHR) |

### 3.2. Measuring devices

For the research, the Sonopan DSA-50 digital sound analyzer was used. The adopted Class 1 meter is compliant with the requirements of PN-EN 61672-1 and has a built-in spectrum analyzer meeting the PN-EN 61260 standard for Class 1 octave and 1/3-octave filters [31]. The analyzer allows measurement of the A-weighted equivalent sound level $L_{Aeq}$ and additional parameters of the Fast, Slow, and Impulse type. The dynamic range of measurements is within the range of 18-135 dB(A) [31]. In the research, a 1/2" measurement microphone characterized by a low level of intrinsic noise and high parameter stability in the range of 20 Hz-20 kHz [31] was used. During the conduct of the research, recording was carried out in the 1/3-octave analyzer mode. At a further stage of the research, the data were exported for further numerical processing. In the case of meters with Class 1 accuracy according to the stated standards, the total indication error of the meter (including the microphone-preamplifier, A/D converter, and digital-filter path) is within the range permitted by the standard, typically of the order of ±1 dB [31]. This error concerns indications at the control points of the frequency and level characteristics. The linearity of the measurement path over the entire dynamic range and the accuracy of the 1/3-octave filters allow an accurate analysis of the distribution of acoustic energy as a function of frequency [31].

It is assumed in this type of research that the sources of measurement uncertainty include: tolerances of the microphone frequency response characteristic, error of the A-weighting characteristic, nonlinearity of the measurement path at high sound levels, the influence of ambient external temperature and humidity, and uncertainty associated with the positioning of the measurement point relative to the source. An additional component of uncertainty is the uncertainty resulting from the sampling time and averaging of the signal in determining L_Aeq. In order to reduce systematic uncertainty, before each measurement series acoustic calibration was carried out using a Class 1 calibrator. The external temperature during the measurements was approximately 4 °C. Taking into account the meter class and the calibration procedure, the total expanded uncertainty of the sound level measurement in the research was approximately ±1–1.5 dB. This is a value acceptable for comparative analyses of spectra and noise levels in the investigated helicopter rotor system.

Figure 9. Carrying out measurements of the equivalent sound level $L_{\mathrm{Aeq}}$, the A-weighted level with Slow time weighting $L_{AS}$, and the 1/3-octave acoustic spectrum for the rotor head without blades.

The figures present the test stand and the successive stages of carrying out the acoustic measurements of the Wabik helicopter rotor. Figures 9 and 10 present the method of conducting measurements of the A-weighted equivalent sound level $L_{Aeq}$, the A-weighted Slow time-weighted level $L_{AS}$, and the acoustic spectrum in 1/3-octave bands for the rotor head without installed blades, respectively in general view and side view. Figure 11 presents the installed rotor blades before the start of the proper measurements, whereas Figure 12 shows the rotor head with the blades set in the neutral position. Figure 13 presents the carrying out of acoustic measurements for the rotor with installed blades over the full operating range of the DLE-170 piston engine. The presented photographic documentation illustrates the configuration of the measurement stand and the conditions of conducting the research.

Figure 10. Carrying out measurements of the equivalent sound level $L_{\mathrm{Aeq}}$, the A-weighted level with Slow time weighting $L_{AS}$, and the 1/3-octave acoustic spectrum for the rotor head without blades – side view.

Figure 11. View of the installed rotor blades of the Wabik helicopter before carrying out the measurements.

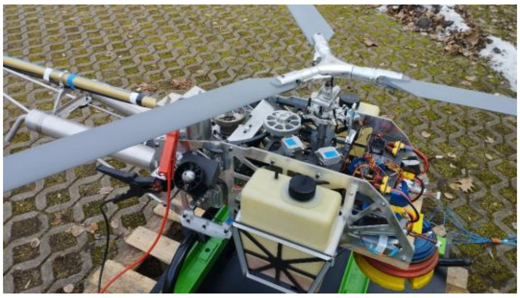

Figure 12. View of the rotor head of the Wabik helicopter with installed blades – neutral state.

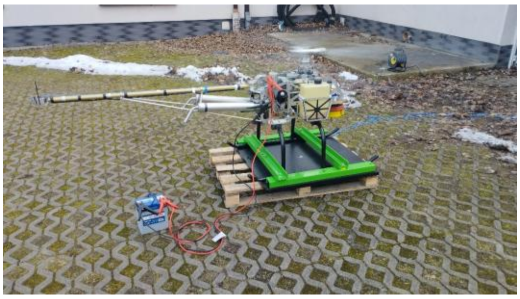

Figure 13. Carrying out measurements of the equivalent sound level $L_{Aeq}$, the A-weighted level with Slow time weighting $L_{AS}$, and the 1/3-octave acoustic spectrum for the installed rotor blades over the full operating range of the DLE-170 piston engine.

### 3.3. Computational procedures

In the investigations and the analysis of noise emissions, the following parameters were used: the A-weighted equivalent sound level $L_{Aeq}$ and the instantaneous level with Slow time weighting, $L_{AS}$. From the general definitions, the equivalent sound level is the level of a constant signal which, during the measurement time T, carries the same acoustic energy as the actual, time-varying noise signal. This relationship can be presented by means of the formula [12]:

$$L_{Aeq,T} = 10\log_{10}\left(\frac{1}{T}\int_0^T \left(\frac{p_A(t)}{p_0}\right)^2 dt\right) \tag{1}$$

where: $p_A(t)$ denotes the instantaneous acoustic pressure after A-weighting, $p_0$ is the reference pressure, a coefficient adopted internationally as the threshold of audibility for the human ear at a frequency of approximately 1 kHz, and T is the measurement time.

The use of the A-weighting filter during the measurements allows the characteristics of human-hearing sensitivity to be taken into account. The adoption of this filter is particularly significant in the analysis of the detectability of small aircraft. The parameter $L_{AS}$ concerns primarily the A-weighted level with the Slow time constant (Slow ≈ 1 s) [13]. In the conducted investigations, $L_{Aeq}$ was used for the energetic analysis of noise emission over the specified measurement time, whereas $L_{AS}$ was used for the assessment of the temporal stability of rotor-system operation at the moment of measurement.

Since the sound level expressed in decibels has a logarithmic character, the use of an ordinary arithmetic mean for averaging measurement results during experimental investigations is not permissible. From the definition of the energy level, this can be expressed by the formula [32]:

$$L = 10\log_{10}\left(\frac{I}{I_0}\right) \tag{2}$$

This means that the linear quantity (energy, intensity) is related to the level in dB by the relationship:

$$\frac{I}{I_0} = 10^{L/10} \tag{3}$$

In order to obtain a correct representative value for three repetitions of the measurement under the same external conditions, it is necessary to use the linear scale, calculate the mean energy, and then use the logarithmic scale. Therefore, for three measurements $L_1, L_2, L_3$, the energetic mean takes the form [32]:

$$L_{avg} = 10\log_{10}\left(\frac{10^{L_1/10}+10^{L_2/10}+10^{L_3/10}}{3}\right) \tag{4}$$

The application of this procedure ensures that the calculated result corresponds to the actual mean acoustic energy emitted by the rotor system. Assuming this relationship, for $N$repetitions of the measurement, the energetic mean is equal to [32]:

$$L_{avg} = 10\log_{10}\left(\frac{1}{N}\sum_{i=1}^{N} 10^{L_i/10}\right) \qquad (5)$$

In the case of the absence of part of the data, e.g. some bands were not recorded because they did not occur, particularly in the lower frequency range, the calculations were performed for the number of available results k. Similar operations were performed for the parameter "Sum", which is the overall A-weighted level (overall) given by the meter. In some measurements, the absence of the value at 25 Hz occurs; this results from measurement limitations and the manner of operation of A-weighting filtration. The applied A-curve attenuates low frequencies very strongly, particularly below 31.5 Hz.

### 3.4. Theoretical premise of the experiment

The fundamental theoretical premise adopted in this study is that, for a rotor system with unchanged geometry, a constant measurement distance, and comparable atmospheric conditions, an increase in rotor-head rotational speed results in a simultaneous increase in the blade-passing frequency and blade-tip speed. According to aeroacoustic theory, the tonal components associated with the blade-passing frequency and its harmonics should shift in accordance with the imposed rotational speed. It is also assumed that the broadband aerodynamic noise generated by the moving blades should increase as a result of higher local flow velocity, pressure fluctuations, and vortex-shedding phenomena occurring near the blade surfaces and blade tips.

For the three-bladed rotor used in the Wabik helicopter, the blade-passing frequency is defined as $f_{BPF} = z \times n/60$, where z is the number of blades and n is the rotor speed expressed in revolutions per minute. Therefore, for n = 1000, 1250, and 1500 RPM, the theoretical blade-passing frequencies are 50.0 Hz, 62.5 Hz, and 75.0 Hz, respectively. These values define the expected positions of the fundamental tonal components, whereas the higher harmonics $m \times f_{BPF}$ should occur at integer multiples of the fundamental frequency. This relationship provides a direct physical justification for performing the analysis in 1/3-octave bands, because this approach enables simultaneous observation of the fundamental rotor tones, their harmonics, and the broadband contribution over the entire measured frequency range.

Furthermore, increasing the rotational speed also increases the angular velocity Ω = 2πn/60 and the blade-tip speed $V_{tip} = \Omega \times R$, which in turn increases the blade-tip Mach number $M_{tip} = V_{tip}/a$ and changes the Reynolds number of the flow around the blade sections. Consequently, both the amplitude and the distribution of acoustic energy in the spectrum should depend not only on the frequency location of the tonal lines, but also on the aerodynamic loading of the rotor. This premise provides the theoretical basis for comparing two test configurations: a rotating rotor head without blades, used to isolate the mechanical noise of the drive and transmission system, and the complete rotor with installed blades, used to determine the additional aerodynamic contribution generated by the rotating blades.

Therefore, the experimental stand was designed to verify whether the expected increase in blade-passing frequency, harmonic content, and broadband aerodynamic noise is reflected in the measured values of $L_{\mathrm{Aeq}}$, $L_{\mathrm{AS}}$, and the 1/3-octave spectra for three controlled rotor-head speeds. Thus, the experiment constitutes a direct verification of the aeroacoustic premise that an increase in rotor angular velocity causes a nonlinear increase in total acoustic emission and changes the spectral structure of the emitted sound.

The generalized analytical relationship describing the expected acoustic response of the rotor system is presented below:

$$L_{A,eq}(n) = 10\log_{10}\left[\frac{1}{p_0^2}\int_0^\infty W_A(f)\left(\sum_{m=1}^{M} A_m(n,\theta)\delta\big(f - mf_{BPF}(n)\big) + S_{bb}(f,n)\right)df\right] \qquad (6)$$

where:

$$A_m(n,\theta) = \Gamma_m M_{tip}(n)^{\alpha_m} Re(n)^{\beta_m} \Phi_m(\theta) \qquad (7)$$

where: $W_A(f)$ is the A-weighting function, $p_0$ is the reference acoustic pressure, $A_m(n,\theta)$ is the energetic coefficient of the *m*-th tonal component dependent on rotor speed and radiation direction, $\Gamma_m$ is the amplitude coefficient of the *m*-th harmonic, $M_{tip}$ is the blade-tip Mach number, $Re$ is the

Reynolds number, $\alpha_m$ and $\beta_m$ are empirical exponents describing the influence of Mach and Reynolds numbers on the tonal component, $\Phi_m(\theta)$ is the acoustic directivity function, $\delta(\cdot)$ denotes the Dirac delta function used to represent tonal components located at harmonics of the blade-passing frequency, $f_{BPF}(n)$ is the blade-passing frequency as a function of rotor speed, and $S_{bb}(f,n)$ is the broadband aerodynamic-noise spectrum. The relationship should be interpreted as a generalized phenomenological representation of the expected acoustic response of the rotor system, not as a closed-form predictive model.

Figure 14 presents one comprehensive block diagram integrating the theoretical premise, the investigated rotorcraft system, the measurement chain, the experimental procedure, the data-processing stage, and the assessment of result reliability.

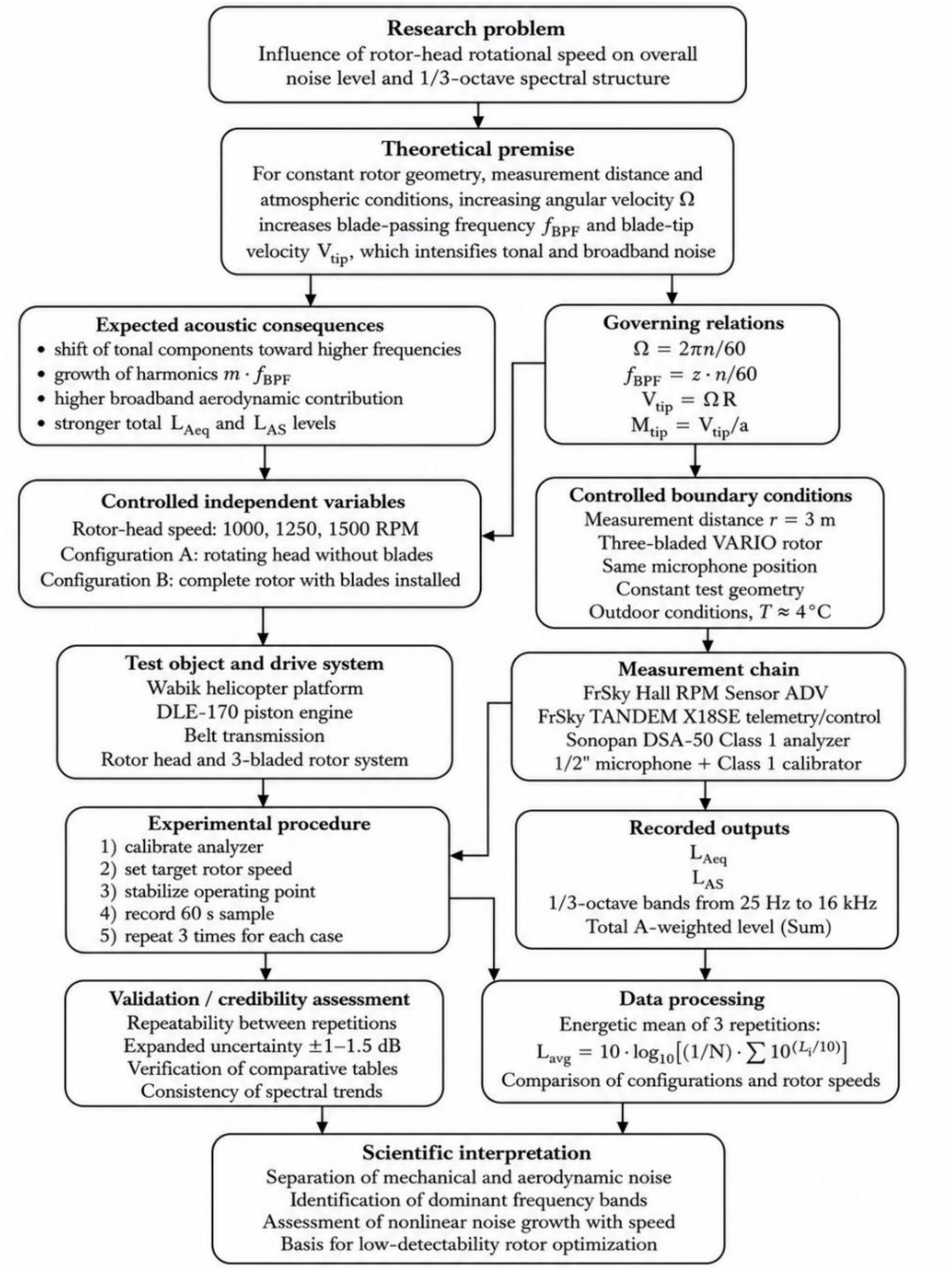


Figure 14. Expanded block diagram of the research procedure and device structure.

## 4. Research result and discussion

For the configuration in which the DLE-170 reciprocating internal combustion engine operated at idle speed of approximately 850 RPM, while the rotor head was not rotating and the rotor blades were not installed, a stable broadband noise spectrum typical of a two-cylinder reciprocating engine without the contribution of a rotor-related aerodynamic component was recorded (Figs. 15–17). The overall sound level in the three repetitions amounted respectively to 77.3 dB, 78.1 dB, and 77.8 dB for $L_{Aeq}$. For the parameter $L_{AS}$, values of 77.7 dB, 78.2 dB, and 78.2 dB were obtained. The differences between $L_{Aeq}$ and $L_{AS}$ do not exceed 0.3–0.4 dB, which confirms the steady character of the emission and the correct operation of the propulsion engine.

The analysis of the 1/3-octave spectrum presented in Figs. 15–17 indicates that the energy maximum occurs in the range of medium frequencies 800 Hz–2 kHz, where the levels reach approximately 66–70 dB. This range corresponds to the dominant harmonics of engine operation and to the resonances of structural elements. In the low-frequency band (25–63 Hz), the levels are distinctly lower and fall within the range of approximately 18–44 dB, with the lowest values concerning 25 Hz, strongly attenuated by the A-filter. In the high-frequency range (6.3–16 kHz), a gradual decrease in the level to approximately 53–63 dB is observed. Such values show the absence of intensive turbulent phenomena.

Figs. 18-20 present three repetitions of the measurement of $L_{Aeq}$ and $L_{AS}$ for the operating helicopter drive in the configuration without rotor blades, at an engine rotational speed of approximately 4000 RPM and a head rotational speed of approximately 1000 RPM. The overall $L_{Aeq}$ level amounted respectively to 81.3 dB, 81.5 dB, and 82.4 dB, whereas $L_{AS}$ amounted to 80.9 dB, 81.9 dB, and 83.7 dB. The energetic mean from the three measurements is 81.76 dB for $L_{Aeq}$ and 82.32 dB for $L_{AS}$. The variability of the overall level between repetitions falls within the range of 1.1 dB for $L_{Aeq}$ and 2.8 dB for $L_{AS}$, which indicates greater dynamics of instantaneous changes in comparison with the idle condition at which the propulsion engine operated. The analysis of the 1/3-octave spectrum shows an energy maximum in the 6.3 kHz band (approx. 72.0-72.8 dB), and elevated levels also occur in the 2-2.5 kHz and 5 kHz bands (approximately 71 dB), as well as in the 800 Hz–1 kHz band (approximately 70.5 dB). In the range 25-63 Hz, the levels are significantly lower (approx. 23-44 dB), which clearly indicates the absence of dominant low-frequency components. Due to the absence of rotor blades, the aerodynamic component is not dominant, whereas the increased energy in the range of several kHz is associated primarily with the mechanical noise of the head drive and power transmission elements at a higher engine rotational speed.

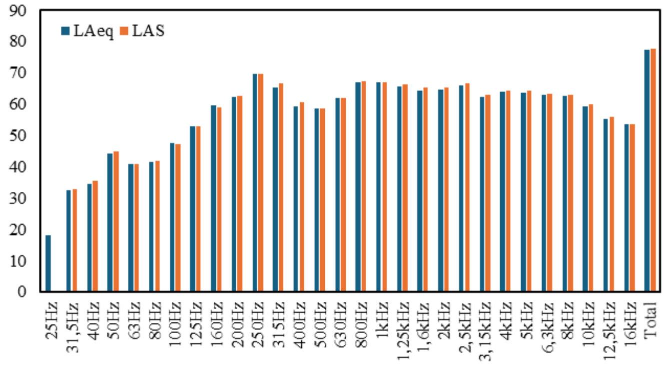


Figure 15. Measurement of $L_{Aeq}$ and $L_{AS}$ for the operating helicopter drive at engine idle speed of approximately 850 RPM, with the rotor head not rotating and without rotor blades installed (measurement 1, duration 60 seconds, distance 3 m).

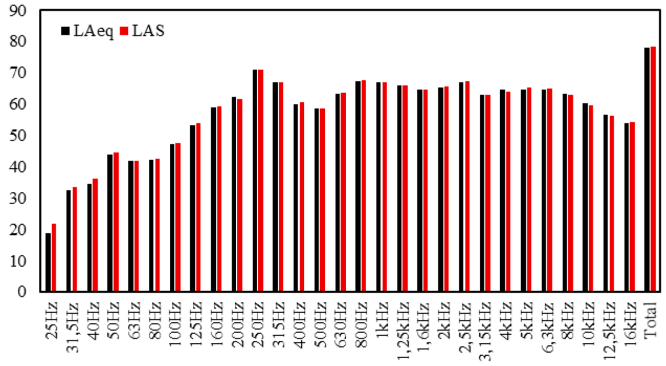


Figure 16. Measurement of $L_{Aeq}$ and $L_{AS}$ for the operating helicopter drive at engine idle speed of approximately 850 RPM, with the rotor head not rotating and without rotor blades installed (measurement 2, duration 60 seconds, distance 3 m).

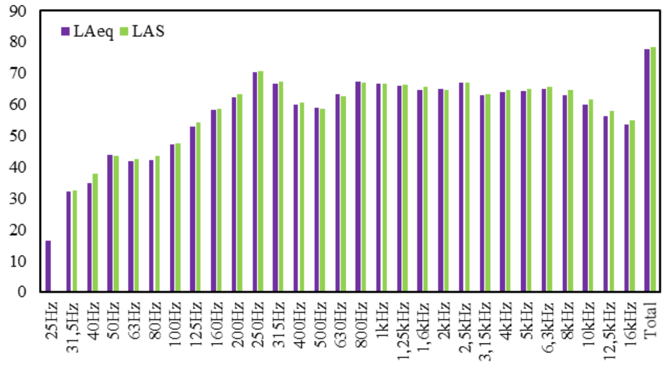


Figure 17. Measurement of $L_{Aeq}$ and $L_{AS}$ for the operating helicopter drive at engine idle speed of approximately 850 RPM, with the rotor head not rotating and without rotor blades installed (measurement 3, duration 60 seconds, distance 3 m).

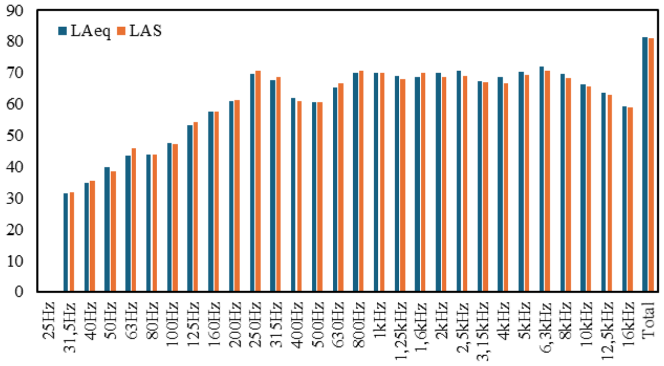


Figure 18. Measurement of L_Aeq and L_AS for the operating helicopter drive without the rotor installed for the rotor head rotational speed range of approximately 1000 RPM – engine approximately 4000 RPM (measurement 1, duration 60 seconds, distance 3 m).

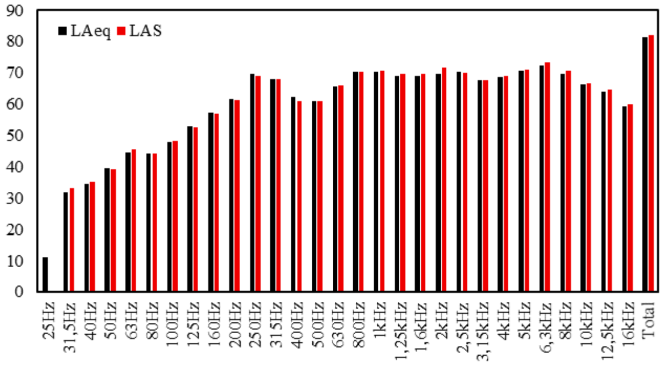


Figure 19. Measurement of $L_{Aeq}$ and $L_{AS}$ for the operating helicopter drive without the rotor installed for the rotor head rotational speed range of approximately 1000 RPM – engine approximately 4000 RPM (measurement 2, duration 60 seconds, distance 3 m).

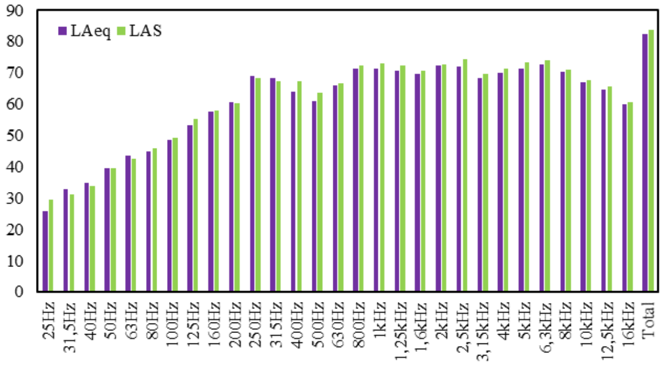


Figure 20. Measurement of $L_{Aeq}$ and $L_{AS}$ for the operating helicopter drive without the rotor installed for the rotor head rotational speed range of approximately 1000 RPM – engine approximately 4000 RPM (measurement 3, duration 60 seconds, distance 3 m).

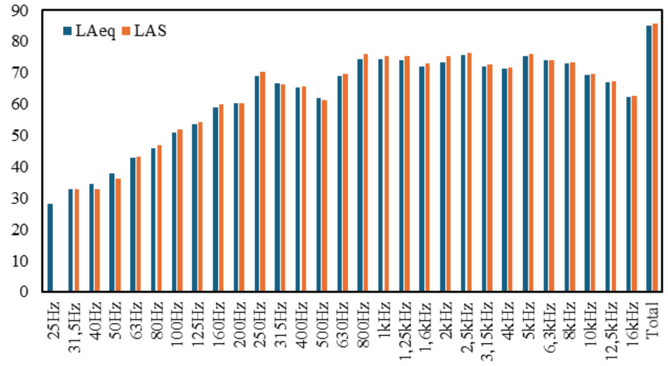


Figure 21. Measurement of $L_{Aeq}$ and $L_{AS}$ for the operating helicopter drive without the rotor installed for the rotor head rotational speed range of approximately 1250 RPM – engine approximately 5000 RPM (measurement 1, duration 60 seconds, distance 3 m).

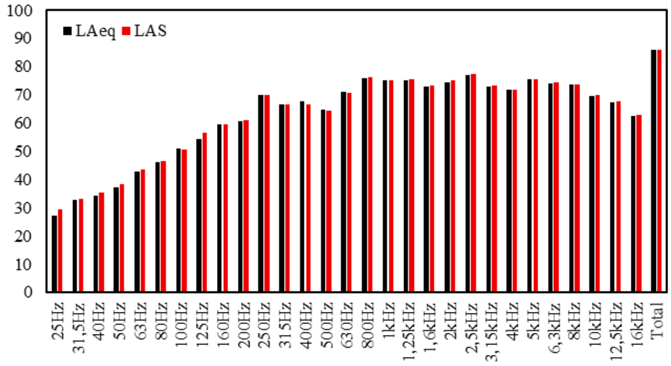


Figure 22. Measurement of $L_{Aeq}$ and $L_{AS}$ for the operating helicopter drive without the rotor installed for the rotor head rotational speed range of approximately 1250 RPM - engine approximately 5000 RPM (measurement 2, duration 60 seconds, distance 3 m).

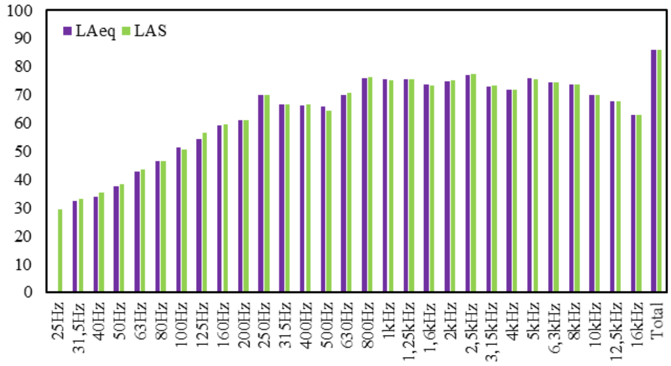


Figure 23. Measurement of $L_{Aeq}$ and $L_{AS}$ for the operating helicopter drive without the rotor installed for the rotor head rotational speed range of approximately 1250 RPM – engine approximately 5000 RPM (measurement 3, duration 60 seconds, distance 3 m).

In Figs. 21-23, three repetitions of the measurement of $L_{Aeq}$ and $L_{AS}$ are presented for the operating helicopter drive in the configuration without rotor blades, at an engine rotational speed of approximately 5000 RPM and a head rotational speed of approximately 1250 RPM. The overall $L_{Aeq}$ level amounted to 84.9 dB, 85.8 dB, and 85.9 dB, whereas $L_{AS}$ amounted to 85.7 dB, 86.0 dB, and 86.3 dB. The energetic mean from the three measurements is 85.56 dB for $L_{Aeq}$ and 86.01 dB for $L_{AS}$, with a small difference between $L_{Aeq}$ and $L_{AS}$ (0.45 dB), which confirms the steady character of the noise emission and the good repeatability of the results. The analysis of the 1/3-octave spectrum indicates an energy maximum in the 2.5 kHz band (approx. 75.8-77.1 dB), and elevated levels are also maintained in the 800 Hz-1.25 kHz bands and in the vicinity of 5 kHz (approximately 75-76 dB). In the low-frequency range (25-63 Hz), the levels remain clearly lower (approx. 28–43 dB), whereas in the range 6.3-16 kHz, a significant energy content is observed (approx. 63–74 dB). This shows the dominant character of the mechanical components of the drive and power transmission system in the absence of the aerodynamic component (absence of blades).

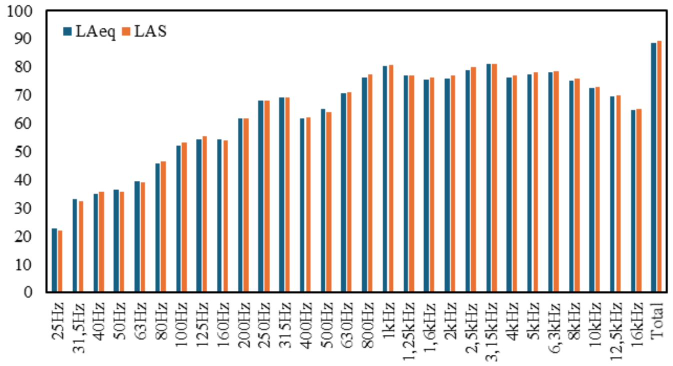


Figure 24. Measurement of $L_{Aeq}$ and $L_{AS}$ for the operating helicopter drive without the rotor installed for the rotor head rotational speed range of approximately 1500 RPM – engine approximately 6000 RPM (measurement 1, duration 60 seconds, distance 3 m).

Figs. 24–26 describe three repetitions of the measurement of $L_{Aeq}$ and $L_{AS}$ for the operating reciprocating internal combustion engine of the helicopter drive in the configuration without rotor blades, at an engine speed of approximately 6000 RPM and a head speed of approximately 1500 RPM – the head rotates. The overall $L_{Aeq}$ level amounted to 88.7 dB, 88.2 dB, and 87.9 dB, whereas $L_{AS}$ amounted to 89.3 dB, 88.2 dB, and 88.5 dB. The energetic mean from the three measurements is 88.28 dB for $L_{Aeq}$ and 88.69 dB for $L_{AS}$, with a difference below 0.5 dB. This indicates very repeatable and stable measurement conditions. This allows the acoustic characteristic to be determined precisely and increases the credibility of the results. The analysis of the 1/3-octave spectrum describes a maximum in the 800 Hz band (79.5 dB) and very high levels in the range 1–3.15 kHz (approximately 78–79 dB). In the low-frequency range, the levels remain significantly lower (26–41 dB), whereas in the high band (6.3–16 kHz) a considerable energy content is observed (64–78 dB).

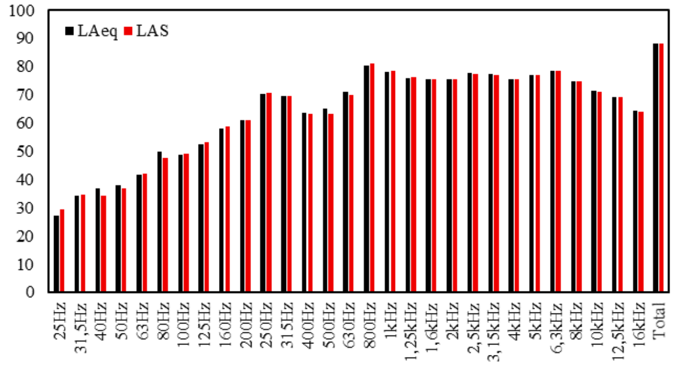


Figure 25. Measurement of $L_{Aeq}$ and $L_{AS}$ for the operating helicopter drive without the rotor installed for the rotor head rotational speed range of approximately 1500 RPM – engine approximately 6000 RPM (measurement 2, duration 60 seconds, distance 3 m).

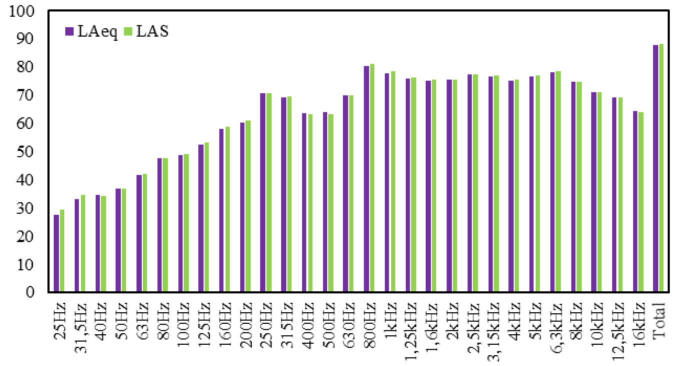


Figure 26. Measurement of $L_{Aeq}$ and $L_{AS}$ for the operating helicopter drive without the rotor installed for the rotor head rotational speed range of approximately 1500 RPM – engine approximately 6000 RPM (measurement 3, duration 60 seconds, distance 3 m).

An increase in the rotational speed of the rotor head from 1000 RPM to 1500 RPM and from 4000 RPM to 6000 RPM (DLE-170 engine) caused an increase in the mean overall $L_{Aeq}$ level from 81.76 dB to 88.28 dB, i.e. by approximately +6.5 dB, which corresponds to more than a fourfold increase in acoustic energy. In comparison with the case of 1250 RPM (85.56 dB), the increase amounts to approximately +2.7 dB, which confirms the nonlinear character of the relationship between the noise level and the rotational speed of the rotor head and engine. Additionally, the spectrum maximum shifts from 6.3 kHz (1000 RPM) through 2.5 kHz (1250 RPM) to 800 Hz (1500 RPM). This indicates a change in the dominant mechanical components with increasing rotational speed of the crankshaft. This means that at the highest rotational speed of the head, the contribution of medium-frequency components increases, which are of the greatest significance from the point of view of auditory perception. This is a particularly important observation for the optimization of the structure and the reduction of its detectability under combat conditions.

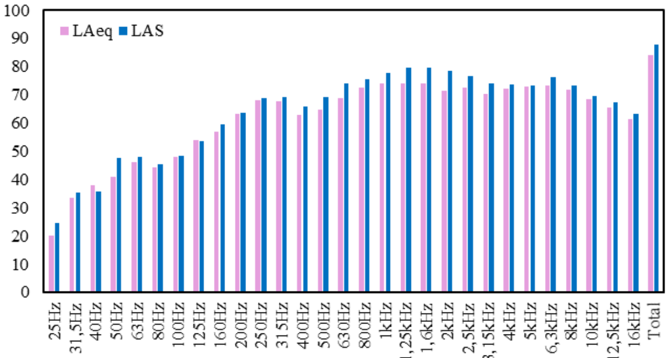


Figure 27. Measurement of $L_{Aeq}$ and $L_{AS}$ for the operating helicopter drive with the rotor installed for the rotor rotational speed range (engaged) of approximately 1000 RPM – engine approximately 4000 RPM (measurement 1, duration 60 seconds, distance 3 m).

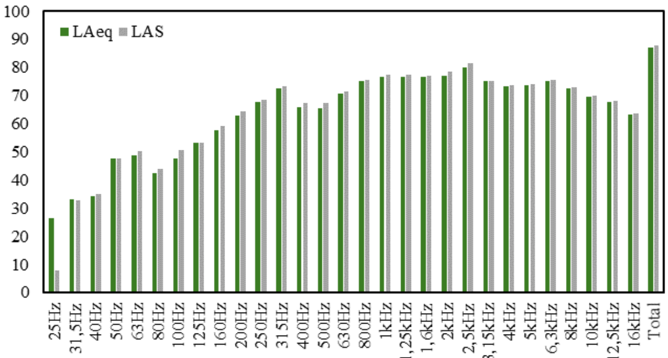


Figure 28. Measurement of $L_{Aeq}$ and $L_{AS}$ for the operating helicopter drive with the rotor installed for the rotor rotational speed range (engaged) of approximately 1000 RPM – engine approximately 4000 RPM (measurement 2, duration 60 seconds, distance 3 m).

In the subsequent stage of the investigations, the overall $L_{Aeq}$ and $L_{AS}$ levels and a very detailed analysis of the 1/3-octave spectrum were presented for the operating engine of the Wabik helicopter with the rotor blades installed for rotor head speeds of 1000 RPM, 1250 RPM, and 1500 RPM. In Figs. 27–29, three repetitions of the measurement of $L_{Aeq}$ and $L_{AS}$ are presented for the operating helicopter drive with the rotor blades installed at an engine speed of approximately 4000 RPM and a head speed of approximately 1000 RPM. The overall $L_{Aeq}$ level amounted to 84.0 dB, 87.1 dB, and 87.6 dB, whereas $L_{AS}$ amounted to 87.8 dB, 87.9 dB, and 88.2 dB. The energetic mean from the three measurements is 86.50 dB for $L_{Aeq}$ and 87.97 dB for $L_{AS}$ . The difference between $L_{Aeq}$ and $L_{AS}$ (1.47 dB) indicates greater instantaneous variability of the signal in comparison with the configuration without blades, which is characteristic of the aerodynamic noise of the rotor. This is important practical information. The analysis of the 1/3-octave spectrum presents an energy maximum in the 2.5 kHz band (78.6 dB) and high levels in the range 1–2 kHz (approximately 76 dB). In the low-frequency range, the levels remain clearly lower (27–49 dB), whereas in the 6.3–16 kHz band a significant energy content is observed (63–75 dB). In contrast to the configuration without blades, the spectrum shows a distinct amplification of the mid-frequency band. This unequivocally confirms the dominance of the aerodynamic component generated by the rotating rotor of the Wabik helicopter.

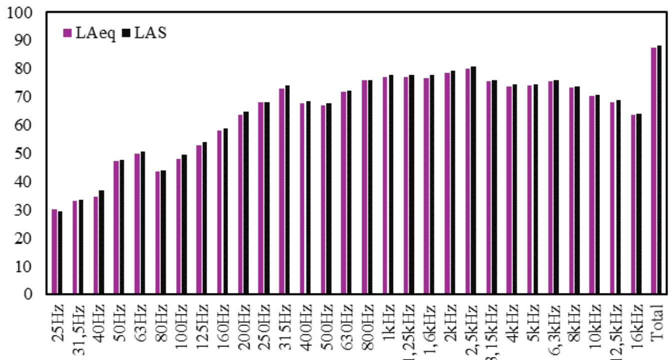


Figure 29. Measurement of $L_{Aeq}$ and $L_{AS}$ for the operating helicopter drive with the rotor installed for the rotor rotational speed range (engaged) of approximately 1000 RPM – engine approximately 4000 RPM (measurement 3, duration 60 seconds, distance 3 m).

Figs. 30–32 describe three repetitions of the measurement of $L_{Aeq}$ and $L_{AS}$ for the operating helicopter drive with the rotor blades installed at an engine speed of approximately 5000 RPM and a head speed of approximately 1250 RPM. The overall $L_{Aeq}$ level amounted to 91.5 dB, 92.6 dB, and 93.3 dB, whereas $L_{AS}$ amounted to 93.0 dB, 92.8 dB, and 94.1 dB. The energetic mean from the three measurements is 92.53 dB for $L_{Aeq}$ and 93.34 dB for $L_{AS}$. The 1/3-octave spectrum shows a maximum in the 1 kHz band (84.74 dB) and very high levels in the 2.5 kHz (84.70 dB) and 3.15 kHz (83.46 dB) bands. The obtained levels (approx. 93 dB) mean that during the tests in this configuration it is necessary to use hearing protectors and maintain an appropriate safety zone around the test stand. Since the spectrum maximum falls in the vicinity of 1–3 kHz, i.e. the band of the greatest sensitivity of human hearing, the noise is very burdensome subjectively and potentially easy to detect under field conditions. This is very important practical information for determining the optimum operating parameters of the aircraft under combat conditions.

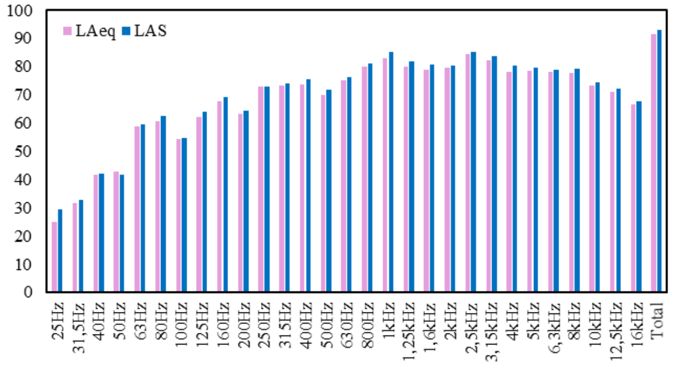


Figure 30. Measurement of $L_{Aeq}$ and $L_{AS}$ for the operating helicopter drive with the rotor installed for the rotor rotational speed range (engaged) of approximately 1250 RPM – engine approximately 5000 RPM (measurement 1, duration 60 seconds, distance 3 m).

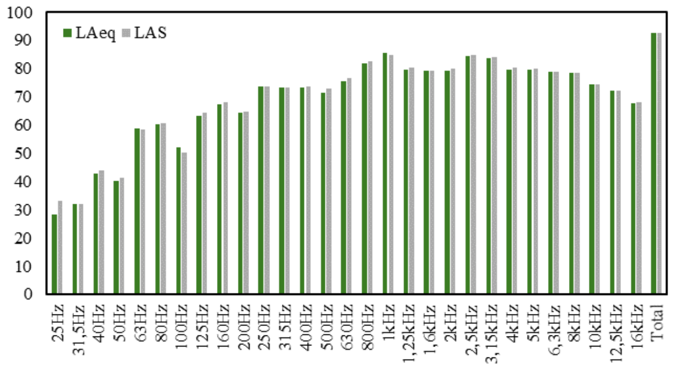


Figure 31. Measurement of $L_{Aeq}$ and $L_{AS}$ for the operating helicopter drive with the rotor installed for the rotor rotational speed range (engaged) of approximately 1250 RPM – engine approximately 5000 RPM (measurement 2, duration 60 seconds, distance 3 m).

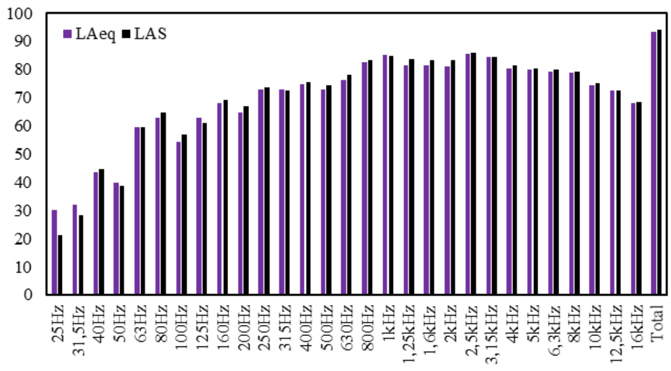


Figure 32. Measurement of $L_{Aeq}$ and $L_{AS}$ for the operating helicopter drive with the rotor installed for the rotor rotational speed range (engaged) of approximately 1250 RPM – engine approximately 5000 RPM (measurement 3, duration 60 seconds, distance 3 m).

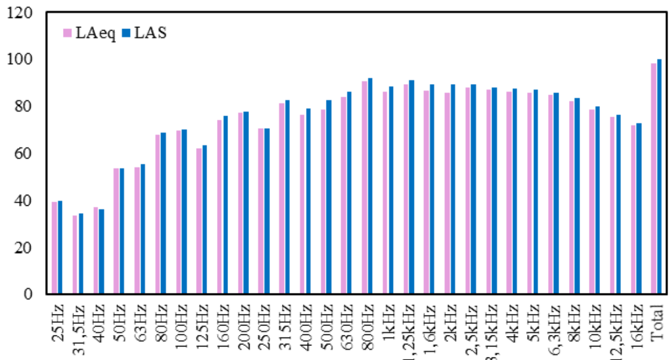


Figure 33. Measurement of $L_{Aeq}$ and $L_{AS}$ for the operating helicopter drive with the rotor installed for the rotor rotational speed range (engaged) of approximately 1500 RPM – engine approximately 6000 RPM (measurement 1, duration 60 seconds, distance 3 m).

In Figs. 33–35, three repetitions of the measurement of $L_{Aeq}$ and $L_{AS}$ are presented for the operating helicopter drive with the rotor blades installed at an engine speed of approximately 6000 RPM and a head speed of approximately 1500 RPM. The overall $L_{Aeq}$ level amounted to 98.1 dB, 98.2 dB, and 99.0 dB, whereas $L_{AS}$ amounted to 99.8 dB, 97.4 dB, and 99.0 dB. The energetic mean amounts to 98.45 dB for $L_{Aeq}$ and 98.84 dB for $L_{AS}$. The 1/3-octave spectrum shows a maximum in the 800 Hz band (90.77 dB) and very high levels in the range 1–3 kHz (87–89 dB). A level of approximately 99 dB means the absolute necessity of using hearing protectors and maintaining an appropriate distance from the test stand. Due to the concentration of energy in the 800 Hz–3 kHz band, the noise is particularly troublesome and propagates well in open terrain, which increases the acoustic detectability of the system. This is valuable practical information concerning the selection of rotor blade geometry and the optimum rotational speed of the engine and rotor head for the Wabik aircraft and similar dual-use helicopter designs.

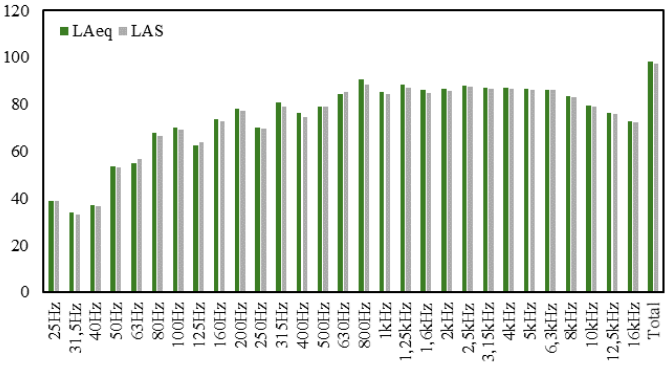


Figure 34. Measurement of $L_{Aeq}$ and $L_{AS}$ for the operating helicopter drive with the rotor installed for the rotor rotational speed range (engaged) of approximately 1500 RPM – engine approximately 6000 RPM (measurement 2, duration 60 seconds, distance 3 m).

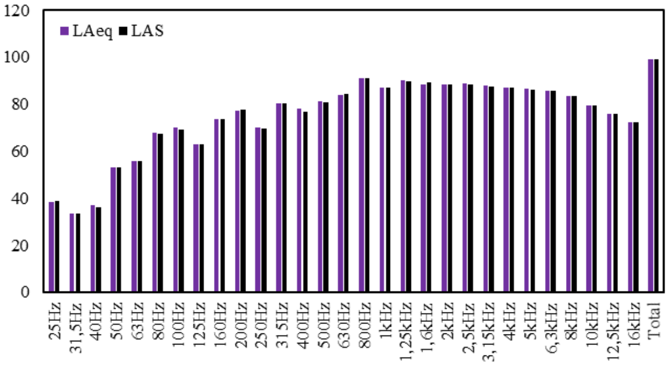


Figure 35. Measurement of $L_{Aeq}$ and $L_{AS}$ for the operating helicopter drive with the rotor installed for the rotor rotational speed range (engaged) of approximately 1500 RPM – engine approximately 6000 RPM (measurement 3, duration 60 seconds, distance 3 m).

At 1000 RPM of the rotor head, the mean $L_{Aeq}$ level was 86.50 dB; at 1250 RPM it increased to 92.53 dB, whereas at 1500 RPM it reached 98.45 dB, which shows a nonlinear, dynamic increase in acoustic energy together with the rotational speed of the engine and rotor head with blades. Increasing the rotational speed of the rotor head from 1000 to 1500 RPM means an increase of approximately +12 dB, i.e. more than a fifteenfold increase in acoustic energy. Together with the increase in speed, the spectrum maximum shifts from the 2.5 kHz band (1000 RPM) and 1 kHz (1250 RPM) toward 800 Hz (1500 RPM), which shows the increasing contribution of aerodynamic components associated with the tip speed of the helicopter rotor blades. At the same time, the level increases in the entire mid-frequency band (0.8–3 kHz), i.e. in the range of the greatest sensitivity of human hearing, which significantly increases the nuisance and acoustic detectability of the design. This information unequivocally indicates the necessity of appropriate selection of the rotational speed of the rotor head and the engine to its gear ratio in such a way as to achieve favourable parameters of engine power and torque distribution while simultaneously obtaining the required thrust force.

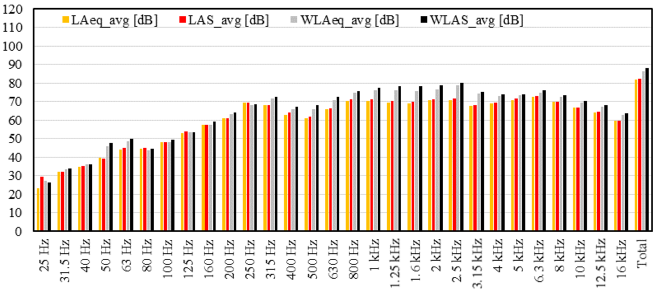


Figure 36. Energetic mean noise spectrum in 1/3-octave bands – comparison of the parameters $L_{Aeq,avg}$ and $L_{AS,avg}$ (without the rotor installed), $WL_{Aeq,avg}$ and $WL_{AS,avg}$ (with the rotor engaged) for approximately 1000 RPM of the rotor head.

The analysis of the 1/3-octave spectra in Fig. 36 indicates that rotor installation causes a distinct increase in the noise level in most frequency bands, particularly in the range of medium and higher frequencies, which affect to the greatest degree the audibility and detectability of the helicopter during flight. In the low-frequency range (25–63 Hz), the differences are moderate. For example, at 25 Hz the $L_{Aeq,avg}$ level increases from 23 dB (without the rotor) to 27.3 dB (with the rotor), i.e. by approximately 4.3 dB. At 63 Hz, the increase amounts to approximately 4.7 dB (from 43.9 dB to 48.6 dB). This means that the rotor also introduces additional energy in the low-tone range, but this is not the dominant range for this propulsion system.

The most significant differences are observed in the medium-frequency band (500 Hz–2.5 kHz). For 800 Hz, the $L_{Aeq,avg}$ level increases from 70.5 dB to 74.7 dB (+4.2 dB). For 1 kHz, the increase amounts to approximately +5.7 dB (from 70.5 dB to 76.2 dB). For 2 kHz, the difference amounts to approximately +5.7 dB (from 70.9 dB to 76.6 dB). In the 2.5 kHz band, the increase reaches approximately +7.6 dB (from 71.0 dB to 78.6 dB). These are differences significant in energetic terms – an increase of 6 dB means approximately a fourfold increase in acoustic power. This indicates that the rotor generates a strong medium-frequency component, which overlaps with the range of the greatest sensitivity of human hearing.

In the high-frequency range (6.3–16 kHz), an increase in level is also observed, although smaller than in the medium band. At 8 kHz, the level increases from 69.9 dB to 72.7 dB (+2.8 dB), and at 16 kHz from 59.6 dB to 62.9 dB (+3.3 dB). The overall sound level ("Total") increases from 81.8 dB (without the rotor) to 86.5 dB (with the rotor) for $L_{Aeq,avg}$, i.e. by 4.7 dB. In the case of $L_{AS,avg}$, the increase is from 82.3 dB to 88.0 dB, i.e. approximately 5.7 dB. Such an increment means more than a threefold increase in the acoustic energy of the whole system after rotor installation. The differences between $L_{Aeq,avg}$ and $L_{AS,avg}$ in both configurations are small (usually below 1 dB). This testifies to the stable character of operation of both the head itself and the system with the rotor – there are no strong impulses or very violent fluctuations. The values of these parameters are particularly important for establishing the controlled flight of the helicopter under combat conditions while maintaining low values of noise emission and sufficient power to transport a warhead or an observation head.

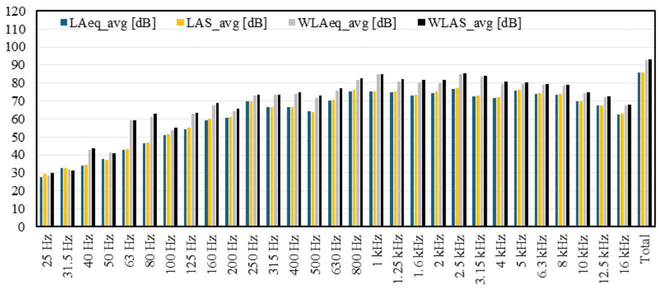


Figure 37. Energetic mean noise spectrum in 1/3-octave bands – comparison of the parameters $L_{Aeq,avg}$ and $L_{AS,avg}$ (without the rotor installed), $WL_{Aeq,avg}$ and $WL_{AS,avg}$ (with the rotor engaged) for approximately 1250 RPM of the rotor head.

The analysis of the 1/3-octave spectra (Figs. 36–38) confirms that an increase in rotor rotational speed results in a systematic increase in the noise level over the entire frequency band. The overall L_(Aeq,avg)level amounts to approximately 86.5 dB for 1000 RPM, 92.5 dB for 1250 RPM, and 98.5 dB for 1500 RPM, which means an increment of approximately 12 dB between 1000 and 1500 RPM, and thus more than a tenfold increase in acoustic energy. The greatest changes are observed in the medium band (800 Hz–2.5 kHz). In the 1 kHz band, the level increases from approximately 70–76 dB (1000 RPM) to 84–85 dB (1250 RPM) and 86–90 dB (1500 RPM), whereas in the 2 kHz band from approximately 71–76 dB to 87–88 dB at 1500 RPM. In the high-frequency range (6.3–16 kHz), the increase amounts to approximately 10–15 dB, which confirms the broadband character of the emission.

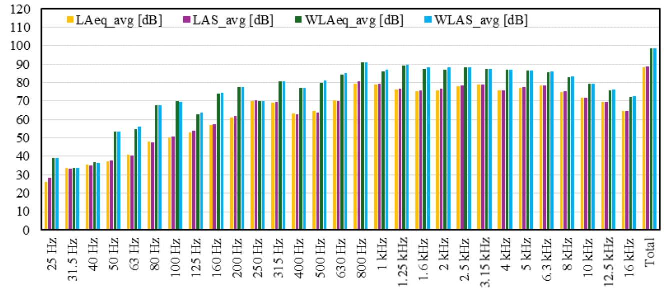


Figure 38. Energetic mean noise spectrum in 1/3-octave bands – comparison of the parameters $L_{Aeq,avg}$ and $L_{AS,avg}$ (without the rotor installed), $WL_{Aeq,avg}$ and $WL_{AS,avg}$ (with the rotor engaged) for 1500 RPM of the rotor head.

The comparison of the configurations with and without the rotor shows that the aerodynamic influence of noise increases together with the rotational speed of the rotor head of the Wabik helicopter. At 1000 RPM, the increase in the overall level amounts to approximately +4.7 dB, at 1250 RPM approximately +6.9 dB, whereas at 1500 RPM approximately +10.2 dB. This means that at the highest analysed speed, the rotor becomes the dominant source of noise. The differences between $L_{Aeq,avg}$ and $L_{AS,avg}$ remain small (usually <1 dB), which indicates the steady, non-impulsive character of the emission.

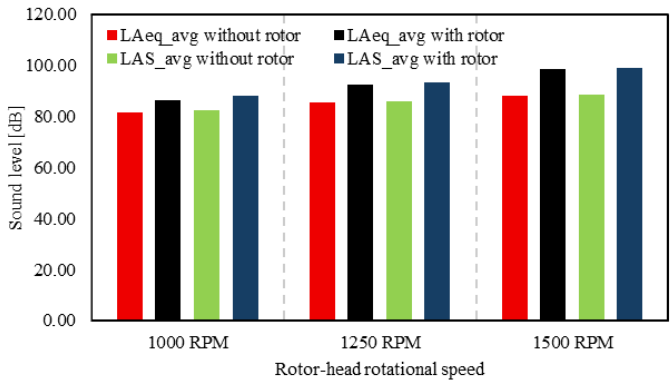


Figure 39. Comparison of overall energetic mean noise levels for different rotor speeds in the Wabik helicopter drive system without rotor blades and with rotor blades installed.

Figure 39 presents comparative values of the overall energetic mean noise levels for different rotor-head rotational speeds: 1000, 1250, and 1500 RPM. The comparison includes both configurations of the Wabik helicopter drive system, i.e.

without installed rotor blades and with the rotor blades installed. The obtained results show that an increase in rotor speed causes a clear increase in the overall noise level, especially in the configuration with the rotor installed. The highest values were recorded at 1500 RPM, which confirms the significant influence of rotor blade operation on the total acoustic emission of the tested system.

### 4.1. Practical implementation

The obtained experimental research results have direct practical significance for selecting the operating range of the rotor propulsion system of the Wabik aircraft. If the mission specification allows it, the propulsion system should operate at the lowest possible rotor rotational speed. This makes it possible to provide the required thrust force and control margin. At a speed of 1000 RPM, the LAeq level with the rotor installed was 86.50 dB, whereas at 1500 RPM it increased to 98.45 dB. This increase of approximately 12 dB corresponds to an almost sixteenfold increase in acoustic energy, and thus directly affects acoustic detectability and operator safety during ground tests.

The most critical frequency range covers 800 Hz–2.5 kHz, where the greatest increases after rotor installation were observed and where human hearing is particularly sensitive. Practical reduction measures should therefore focus on the geometry of the blade tips, the selection of the airfoil, rotor balancing, vibration isolation of the power transmission system, and the selection of the engine-to-rotor gear ratio. Limiting the spectral components in this range is also important for reducing the possibility of passive acoustic detection under operational conditions.

The presented experiment was carried out on a static test stand, without additional payload and without aerodynamic loading resulting from flight. In real flight, the noise level may change because the aircraft payload requires changes in collective pitch, rotor thrust, induced inflow, and engine torque. A higher payload is expected to increase the aerodynamic component of noise and may change the relative contribution of tonal and broadband components. This is almost certain in the range of 800 Hz–2.5 kHz. Therefore, the bench-test results should be treated as a reliable comparative baseline, whereas further flight tests with different payloads are recommended for final operational verification. The results also indicate that spectral analysis should be used together with the assessment of the overall sound level, because the same total level may correspond to different detectability depending on the dominant frequency bands.

The results can also be used during further development of small dual-use rotorcraft and UAV propulsion systems. The comparison of the two configurations shows that the aerodynamic contribution of the blades increases with rotational speed: the installation of the rotor increased LAeq by about 4.7 dB at 1000 RPM, 6.9 dB at 1250 RPM, and 10.2 dB at 1500 RPM compared with the configuration without blades. This confirms that the highest tested speed should be avoided when low acoustic detectability is required, unless mission performance or payload requirements make this operating range necessary.

## 5. Conclusion

The conducted experimental study confirmed that rotor-head rotational speed has a strong and nonlinear influence on the acoustic emission of the prototype Wabik helicopter rotor system. In the configuration without rotor blades, the energetic mean LAeq increased from 81.76 dB at 1000 RPM to 85.56 dB at 1250 RPM and 88.28 dB at 1500 RPM. After installing the rotor blades, the corresponding LAeq values increased to 86.50 dB, 92.53 dB, and 98.45 dB, respectively. Thus, the increase in rotor-head speed from 1000 to 1500 RPM caused a total rise of approximately 12 dB in the complete rotor configuration, which means an almost sixteenfold increase in acoustic energy.

The comparison of the two tested configurations made it possible to separate the mechanical contribution of the hub and drive system from the aerodynamic contribution generated by the blades. At 1000 RPM, rotor installation increased the overall LAeq level by approximately 4.7 dB. At 1250 RPM, this difference increased to approximately 6.9 dB, whereas at 1500 RPM it reached approximately 10.2 dB. This shows that, at the highest analysed rotational speed, the rotor blades become the dominant source of additional noise emission under the tested piston-engine operating conditions.

The 1/3-octave analysis showed that the most important changes occurred in the medium-frequency range. The dominant spectral bands shifted with increasing rotational speed from approximately 2.5 kHz through 1 kHz to 800 Hz, while the

800 Hz-2.5 kHz range became the most significant for detectability and operator exposure. In this range, selected band-level increases reached several decibels after rotor installation, and the total broadband character of the spectrum confirmed that the acoustic impact cannot be reduced only by targeting a single tonal component.

The obtained results provide a quantitative basis for further optimization of the Wabik rotor system. The most effective reduction measures should combine rotor-speed management, blade-tip and airfoil optimization, accurate balancing, and vibration isolation of the drive-transmission system. The results also indicate that operation close to 1000 RPM is acoustically more favourable than operation at 1500 RPM, provided that the required thrust, payload, and safety margins are maintained. Future work should include measurements under real flight conditions, with different payloads and collective-pitch settings, in order to verify how aerodynamic loading changes the noise spectrum and overall emission level.

**References**


1. Bondar K. Ukraine's future vision and current capabilities for waging AI-enabled autonomous warfare. Washington, DC: Center for Strategic and International Studies; 2025.
2. Nieczypor K, Matuszak S. Game of drones: the production and use of Ukrainian battlefield unmanned aerial vehicles. OSW Commentary No. 694. Warsaw: Centre for Eastern Studies; 2025: 1-6.
3. Dumitrescu C, Minea M, Costea IM, Chiva IC, Semenescu A. Development of an acoustic system for UAV detection. *Sensors* 2020; 20(17): 4870. https://doi.org/10.3390/s20174870.
4. Tejera-Berengue D, Zhu-Zhou F, Utrilla-Manso M, Gil-Pita R, Rosa-Zurera M. Acoustic-based detection of UAVs using machine learning: analysis of distance and environmental effects. In: *Proceedings of the 2023 IEEE Sensors Applications Symposium (SAS)*; Ottawa, ON, Canada. Piscataway, NJ: Institute of Electrical and Electronics Engineers; 2023. p. 1-6. https://doi.org/10.1109/SAS58821.2023.10254127.
5. Brążkiewicz D, Mazurek R. Współczesne powietrzne drony rozpoznawczo-bojowe i ich użycie oraz zwalczanie na przykładzie wojny rosyjsko-ukraińskiej. In: Brążkiewicz D, Chodyka M, Grudniewski T, Nowicka J (eds). Wielowymiarowość środowiska bezpieczeństwa. Część pierwsza. Biała Podlaska: Wydawnictwo Akademii Bialskiej im. Jana Pawła II; 2025: 81-104. https://doi.org/10.29316/9788368103199_5.
6. Kang C, Huang Q, Sun F, Liang X, Xu L. From classical approaches to recent advancements: a holistic review of acoustic detection for unmanned aerial vehicles. *AIP Advances* 2025; 15(12): 120701. https://doi.org/10.1063/5.0304975.
7. Wróblewski P, Kiszkowiak Ł, Bratkowski P, Milczarczyk J. Thrust characteristics of the OSA-3 aircraft propulsion system with a two-stroke piston internal-combustion engine for selected propeller configurations. *Advances in Science and Technology Research Journal* 2026; 20(4): 1-21. https://doi.org/10.12913/22998624/211735.
8. Wróblewski P, Kiszkowiak Ł, Milczarczyk J, Bratkowski P. Testing of the sound level produced by a two-stroke piston internal combustion engine mounted on the aircraft depending on the propeller profile. *Advances in Science and Technology Research Journal* 2026; 20(2): 337-360. https://doi.org/10.12913/22998624/211734.
9. Yu YH. Rotor blade-vortex interaction noise. *Progress in Aerospace Sciences* 2000; 36(2): 97-115. https://doi.org/10.1016/S0376-0421(99)00012-3.
10. Yu YH, Gmelin B, Splettstoesser W, Philippe JJ, Prieur J, Brooks TF. Reduction of helicopter blade-vortex interaction noise by active rotor control technology. *Progress in Aerospace Sciences* 1997; 33(9-10): 647-687. https://doi.org/10.1016/S0376-0421(97)00006-7.
11. Męsikowska M. Classification of unmanned aerial vehicles based on acoustic signals obtained in external environmental conditions. *Sensors* 2024; 24(17): 5663. https://doi.org/10.3390/s24175663.
12. International Organization for Standardization. ISO 1996-1:2016. Acoustics—Description, measurement and assessment of environmental noise—Part 1: Basic quantities and assessment procedures, 3rd ed. Geneva: International Organization for Standardization; 2016.
13. International Electrotechnical Commission. IEC 61672-1:2013. Electroacoustics—Sound level meters—Part 1: Specifications, 2nd ed. Geneva: International Electrotechnical Commission; 2013.
14. International Civil Aviation Organization. Annex 16 to the Convention on International Civil Aviation: Environmental Protection. Volume I: Aircraft Noise, 8th ed. Montreal: International Civil Aviation Organization; 2017.
15. International Civil Aviation Organization. Environmental Technical Manual. Volume I: Procedures for the Noise Certification of Aircraft

(Doc 9501-1), 3rd ed. Montreal: International Civil Aviation Organization; 2018.

16. International Civil Aviation Organization. Reduction of Noise at Source. https://www.icao.int/environmental-protection/reduction-noise-source; 2026 [accessed 16 August 2026].
17. Kopeć R, Wasiuta O, Wójtowicz T. Wojna dronów: militarne wykorzystanie bezzałogowych statków powietrznych. Kraków: Wydawnictwo Naukowe Uniwersytetu Pedagogicznego im. Komisji Edukacji Narodowej w Krakowie; 2021. https://doi.org/10.24917/9788380846074.
18. Hung JY, Gonzalez LF. On parallel hybrid-electric propulsion system for unmanned aerial vehicles. *Progress in Aerospace Sciences* 2012; 51: 1-17. https://doi.org/10.1016/j.paerosci.2011.12.001.
19. Wojtas M, Wyszkowski P, Mądro M, Osiewicz M, Kmita P. Test stand for propellers and rotors in VTOL drone systems. *Transactions on Aerospace Research* 2023; 270(1): 67-85. https://doi.org/10.2478/tar-2023-0006.
20. Klimczyk WA. Aerodynamic design and optimization of propellers for multirotor. *Aircraft Engineering and Aerospace Technology: An International Journal* 2022; 94(1): 21-30. https://doi.org/10.1108/AEAT-12-2020-0288.
21. Kozaczuk KJ. Composite technology development based on helicopter rotor blades. *Aircraft Engineering and Aerospace Technology: An International Journal* 2020; 92(3): 273-284. https://doi.org/10.1108/AEAT-12-2017-0260.
22. Wei W, Ma Y, Wei S, Wang D, Guo M, Yan Q. Analysis and evaluation of aerodynamic noise characteristics of toroidal propeller. *Drones* 2024; 8(12): 753. https://doi.org/10.3390/drones8120753.
23. Li Y, Ma Z, Qu R, Tan Q, Zhong S, Zhou P, Zhang X. Effect of rotation speed fluctuation on rotor noise generation: a numerical and experimental study. *Journal of Sound and Vibration* 2025; 595: 118717. https://doi.org/10.1016/j.jsv.2024.118717.
24. Jekateryńczuk G, Piotrowski Z. Outdoor microphone range tests and spectral analysis of UAV acoustic signatures for array development. *Sensors* 2025; 25(22): 7057. https://doi.org/10.3390/s25227057.
25. Steinhoff L, Koschlik AK, Arts E, Soria-Gomez M, Raddatz F, Kunz VD. Development of an acoustic fault diagnosis system for UAV propeller blades. *CEAS Aeronautical Journal* 2024; 15(4): 881-893. https://doi.org/10.1007/s13272-024-00752-8.
26. FrSky Electronic Co., Ltd. TANDEM X18S / X18SE user manual. https://www.frsky-rc.com/download/; 2026 [accessed 16 August 2026].
27. Modele24. FrSky HALL RPM SENSOR ADV. https://modele24.pl/en/other/220-frsky-hall-rpm-sensor-adv.html; 2026 [accessed 16 August 2026].
28. DLEngine Inc. DLE170: technical specifications. https://www.dlengine.com/en/rcengine/dle170/; 2026 [accessed 16 August 2026].
29. KST Servos. X20-12-M-835 HV brushless HLS servo: technical specifications. https://kstservos.com/products/x20-12-m-835-hv-brushless-hls-servo-48kgf-cm-0-14sec-for-rc-helicopters; 2026 [accessed 16 August 2026].
30. VARIO Helicopter. 3-blade-set 2500 mm, Ord. No. 416/3 and 417/3. https://www.vario-helicopter.biz/cn/index.php?cPath=25; 2026 [accessed 16 August 2026].
31. SONOPAN Sp. z o.o. DSA-50 digital sound analyzer: instruction manual. Białystok: SONOPAN Sp. z o.o.; 2012.
32. Bies DA, Hansen CH. Engineering Noise Control: Theory and Practice, 4th ed. London: CRC Press; 2009. https://doi.org/10.1201/9781315273464.